

AD-A181 472

THERMAL OXIDATION OF SILICON: NEW EXPERIMENTAL RESULTS
AND MODELS(U) NORTH CAROLINA UNIV AT CHAPEL HILL DEPT
OF CHEMISTRY E A IRENE ET AL. 03 JUN 87 TR-15

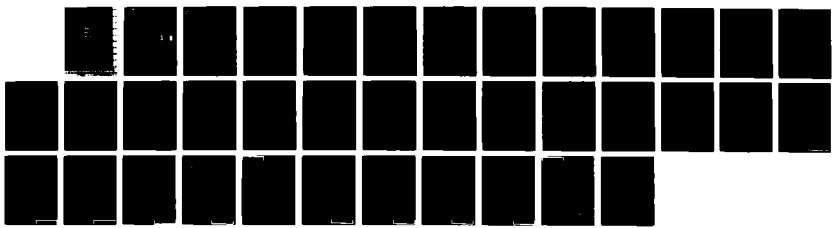
1/1

UNCLASSIFIED

N00014-86-K-0305

F/G 7/4

NL





MICROCOPY RESOLUTION TEST CHART
NATIONAL BUREAU OF STANDARDS-1963-A

AD-A181 472

OFFICE OF NAVAL RESEARCH

CONTRACT NO. N00014-86-K-0305

TECHNICAL REPORT NO. 15

Thermal Oxidation of Silicon: New Experimental Results & Models

E.A. Irene
Department of Chemistry
University of North Carolina
Chapel Hill, NC 27514

and

R. Ghez
IBM Thomas J. Watson Research Center
Yorktown Heights, NY 10598

DTIC
SELECTED
JUN 17 1987
S D

in

Applied Surface Science

Reproduction in whole or in part is permitted for any purpose of the United States Government.

This document has been approved for public release and sale; its distribution is unlimited.

A181472

REPORT DOCUMENTATION PAGE

1a. REPORT SECURITY CLASSIFICATION Unclassified		1b. RESTRICTIVE MARKINGS	
2a. SECURITY CLASSIFICATION AUTHORITY		3. DISTRIBUTION/AVAILABILITY OF REPORT Approved for public release; distribution unlimited.	
2b. DECLASSIFICATION/DOWNGRADING SCHEDULE		4. PERFORMING ORGANIZATION REPORT NUMBER(S) Technical Report #15	
5a. NAME OF PERFORMING ORGANIZATION UNC Chemistry Dept.		5b. OFFICE SYMBOL (If applicable)	
6a. ADDRESS (City, State and ZIP Code) 11-3 Venable Hall 045A Chapel Hill, NC 27514		7a. NAME OF MONITORING ORGANIZATION Office of Naval Research (Code 413)	
6b. NAME OF FUNDING/SPONSORING ORGANIZATION Office of Naval Research		6c. ADDRESS (City, State and ZIP Code) Chemistry Program 800 N. Quincy, Arlington, VA 22217	
7b. ADDRESS (City, State and ZIP Code) Chemistry Program 800 N. Quincy Street Arlington, Virginia 22217		8. PROCUREMENT INSTRUMENT IDENTIFICATION NUMBER Contract #N00014-86-K-0305	
9a. NAME OF FUNDING/SPONSORING ORGANIZATION Office of Naval Research		9b. OFFICE SYMBOL (If applicable)	
10. SOURCE OF FUNDING NOS.		11. TITLE (Include Security Classification) THERMAL OXIDATION OF SILICON: NEW EXPERIMENTAL RESULTS & MODELS	
PROGRAM ELEMENT NO.		PROJECT NO.	
TASK NO.		WORK UNIT NO.	
12. PERSONAL AUTHOR(S) E.A. Irene and R. Ghez			
13a. TYPE OF REPORT Interim Technical		13b. TIME COVERED FROM _____ TO _____	
14. DATE OF REPORT (Yr., Mo., Day) June 3, 1987		15. PAGE COUNT 32	
16. SUPPLEMENTARY NOTATION Prepared for publication in Applied Surface Science.			
17. COSATI CODES		18. SUBJECT TERMS (Continue on reverse if necessary and identify by block number)	
FIELD	GROUP	SUB. GR.	
19. ABSTRACT (Continue on reverse if necessary and identify by block number) <p>Most studies of ^{Silicon} Si oxidation commence with a discussion of the Linear-Parabolic oxidation model developed by a number of workers in the 1960's. The limits of the model are pure diffusion of oxidant for thick ^{silicon dioxide} (SiO₂) films and a surface reaction limitation for thin films. The steady state picture of this series reaction scheme is discussed and used to explain new experimental results. New data relevant to Si oxidation is presented on the following subjects: five orientations of Si; photonic excitement; intrinsic film stress; silicide oxidation. The role of electrons on the oxidation kinetics is elucidated. A thermionic emission model for the initial stages of oxidation is proposed.</p>			
20. DISTRIBUTION/AVAILABILITY OF ABSTRACT UNCLASSIFIED/UNLIMITED <input checked="" type="checkbox"/> SAME AS RPT. <input checked="" type="checkbox"/> DTIC USERS <input type="checkbox"/>		21. ABSTRACT SECURITY CLASSIFICATION Unclassified	
22a. NAME OF RESPONSIBLE INDIVIDUAL Dr. David L. Nelson		22b. TELEPHONE NUMBER (Include Area Code) (202) 696-4410	
		22c. OFFICE SYMBOL	

Thermal Oxidation of Silicon: New Experimental Results and Models

Eugene A. Irene
Dept. of Chemistry
University of North Carolina
Chapel Hill, North Carolina 27514
U. S. A.

and

R. Ghez
IBM Thomas J. Watson Research Center
Box 218
Yorktown Heights, New York 10598
U. S. A.

Accession For	
NTIS CRA&I	<input checked="" type="checkbox"/>
DTIC TAB	<input type="checkbox"/>
Unannounced	<input type="checkbox"/>
Justification	
By	
Distribution /	
Availability Codes	
Dist	Avail and/or Special
A-1	



Abstract

Most studies of Si oxidation commence with a discussion of the Linear-Parabolic oxidation model developed by a number of workers in the 1960's. The limits of the model are pure diffusion of oxidant for thick SiO_2 films and a surface reaction limitation for thin films. The steady state picture of this series reaction scheme is discussed and used to explain new experimental results. New data relevant to Si oxidation is presented on the following subjects: five orientations of Si; photonic excitement; intrinsic film stress; silicide oxidation. The role of electrons on the oxidation kinetics is elucidated. A thermionic emission model for the initial stages of oxidation is proposed.

Introduction

The linear parabolic, L-P, oxidation model(1-4) is typically adopted as the basis from which to describe Si oxidation phenomena. This model is based on a consideration of mass balance and the arrival at the steady state of essentially two rate processes. One of the processes is the transport of oxidant across the SiO₂ film, represented in Figure 1 as F₁, and the other process is the reaction of oxidant with Si at the Si-SiO₂ interface which is shown as F₂. It is intuitive that these processes are essential for oxidation. Which of these processes is kinetically dominant is not intuitive and the subject of numerous experimental investigations. Before specific experimental studies are considered which elucidate this issue, it is useful to consider the implications of mass balance and the steady state.

Diffusion of Oxidant in SiO₂

Fickian diffusion is usually taken to mean that the mass flux, F₁, is proportional to a concentration gradient, dC/dx, which in the steady state is time independent:

$$F_1 = DdC/dx \quad (1)$$

where D, the diffusivity, is the constant of proportionality. A number of concordant studies(5,6) show that the O₂ flux through

SiO₂ is overwhelmingly without interaction with the SiO₂ network. On the other hand, for the case where even traces of H₂O are present the exchange of O with the network is rapid(6,7) and the oxidation kinetics are decidedly altered(8,9). The overall oxidation rate has been shown to scale with oxidant pressure(10,11). These kinds of oxidation studies along with the intuitive idea that as the oxide grows the reactants are increasingly separated, yield the conclusion that the transport of oxidant, or the oxidant supply function is kinetically important.

The Interfacial Reaction

It is clear that SiO₂ cannot form without the reaction of Si and O atoms. The reaction can be expressed in terms of a flux, F_s, where the concentrations of both chemical species are important:

$$F_s = k[O][Si] \quad (2)$$

and where k is a rate constant. Since for a specified crystallographic orientation, the availability of Si atoms on the surface is constant, [Si] could be included in k. However, it is now well established that the oxidation rate is dependent upon the orientation up to thousands of angstroms(12) and thus it is explicit in equation (2). We ignore that [O] and [Si] may appear in equation (2) raised to powers other than unity and that oxygen

molecules, O_2 , may be important.

Series Processes-Mass Balance-Steady State

With the processes of transport of oxidant and subsequent reaction in series, mass balance requires that the fluxes relax to the same value, F , as:

$$F = F_1 = F_2 \quad (3)$$

This relaxation will cause the establishment of a quasi stationary concentration at the Si-SiO₂ interface, C_2 , as:

$$dC_2/dt = 0 \quad (4)$$

This physical picture is shown in Figure 2 after Levich(44) where $F(C_2)$ for both F_1 and F_2 is graphed versus C_2 . It is seen that at the O_2 -SiO₂ interface, the maximum value for F_1 is calculated at $C_2 = 0$ as:

$$F_1(0) = DC_1/L \quad (5)$$

where C_1 is the solubility of oxidant in the SiO₂ and L is the SiO₂ thickness. F_1 goes to 0 at $C_2 = C_1$ and varies linearly in between, hence a straight line is drawn between these extrema in F_1 . F_2 can have any maximum value and is shown with both a larger and smaller maximum value than F_1 . The maximum value for F_2 is at $C_2 = C_1$ and has a value of 0 at $C_2 = 0$. These extrema in F_2 can

be connected by a line. The intersection of the two functions yields the steady state solution for C_2 , viz. the C_2 value that satisfies equation (3) above.

While in general the maximum value for F_2 can be smaller or larger than F_1 , below we show evidence which supports the former. Also, it is seen that the F value obtained from the steady state must be less than the smallest flux, since the intersection for two downwardly sloping lines yields such an intersection. The slope of the F_2 function is determined by k for any value of C_1 , and the slope of F_1 by D . Changes in oxidation rate can be analyzed by noting the changes in the intersection point as a result of changes in the parameters in each flux expression. We will use this idea later to explain some experimental results. Thus Figures 1 and 2 provide pictures of the important overall processes and how these processes interact in series.

Results

The Dominant Rate Process

In order to address the question posed above as to which rate process is dominant, several simple calculations are relevant.

First, a comparison is made of the maximum O_2 diffusive flux (at $C_2 = 0$), $F_1(0)$, with the experimentally obtained oxidation rate converted to an O_2 flux, $F(\text{exp})$. This comparison is easily made by forming a ratio, R , as:

$$R = F_1(0)/F(\text{exp}) \quad (6)$$

Table 1 shows some recently reported values(12,13). Literature values for D(14) and C_1 (3) were used. It is seen that for any reasonable oxide thicknesses, R values considerably greater than unity are found. R values of unity indicate that the reaction scheme is under transport control which is approached for large SiO_2 thicknesses greater than 2000 Å. For R greater than unity, ie. most of the important SiO_2 film thicknesses, $F < F_1(0)$ and this indicates that a steady state value for C_1 is non zero.

Using the D values for O_2 , a random walk calculation shows that the net distance travelled by an O_2 molecule in SiO_2 in one second is quite large and as shown in Table 2 is about 10^4 Å. Thus F_1 appears to be quite large. A recent report (15) has shown that the thermodynamic potential associated with oxidant transport during Si oxidation is smaller than the reaction potential by more than a factor of 50.

Now considering these three calculations and the picture in Figure 2, one can conclude that the observed oxidation rate as F is nearer to the F_2 line. This indicates a large slope for the F_1 line (a large D) and that $F_1 > F_2$ for the maximum values. Experimental support for this is now presented.

The Effect of Si Orientation

It has long been recognized that the different Si

orientations oxidize at differing oxidation rates(2,3,16-18). For the three lowest index major Si orientations, the reported rate order is as follows:

$$\text{Rate}(110) > \text{Rate}(111) > \text{Rate}(100)$$

for steam at 1 atm(2) and

$$\text{Rate}(111) > \text{Rate}(110) > \text{Rate}(100)$$

for high pressure steam oxidation(16). Such differences were accounted for in the L-P model by adjustments in the linear rate constant, k , in equation (2). All the authors agree that the number of Si atoms per area, N_s , is the important parameter and this is shown explicitly in equation (2). N_s was calculated for the three major orientations(16) and found to be in the order:

$$N_s(110) > N_s(111) > N_s(100).$$

Thus for one of the above cited studies (high pressure steam) another parameter was required to be invoked that could dominate the kinetics. This was chosen to be steric factors and a geometric argument was proposed to explain the experimental results(16).

Recent detailed kinetics studies(19-21) using the three major Si orientations, have conclusively shown that for 1 atm dry

O₂ oxidations the initial rate order (less than several hundred A) is:

$$\text{Rate}(110) > \text{Rate}(111) > \text{Rate}(100)$$

which changes for thicker films to the order:

$$\text{Rate}(111) > \text{Rate}(110) > \text{Rate}(100).$$

A model was proposed for the initial order and the "crossover effect"(22). For the initial regime the rate simply scales with N_s, as given above, since the very initial regime ought to be dominated by the interface reaction where :

$$[Si] \propto N_s$$

The crossover, which occurs at greater film thicknesses was attributed to a film stress effect that is manifest as the force which grows with the film thickness. The intrinsic stress develops as a result of the change in molar volume, ΔV , which occurs from the conversion of Si to SiO₂ and is about 120%. The orientation dependence was thought to arise from the application of Hookes law as:

$$\sigma = E\epsilon \quad (7)$$

where σ is the stress, and ϵ is the strain, and is proportional to ΔV , and E is Young's modulus which is orientation dependent.

The variation of E is:

$$E(111) > E(110) > E(100)$$

thus paralleling the order of the oxidation rate, R , above the crossover. The stress is compressive in the oxide, but tensile in the Si surface. This latter stretched bond situation in the Si was considered to be responsible for the enhanced R for the (111) orientation above the crossover. It should be noted that at the time this stress argument was developed, the experimental measurements of SiO_2 stresses on various Si orientations were not available. Recently, a large number of precise SiO_2 film stress measurements have been reported(23,24) which definitely show that the intrinsic stress does not follow the order for E above. In fact, Figure 3 shows that the measured stress on the (111) surface is lower than for the other three orientations which are nearly equal. Thus the stress based model as proposed above cannot be correct. The fact that the (111) measured stress is the lowest with the stresses for the other orientations grouped, suggests an anomaly with only the (111) surface. The smaller compressive oxide stress for SiO_2 on the (111) surface may result in a larger D value for O_2 thereby explaining the increased oxidation rate. It is this idea that is used later to explain the orientation results. Before presenting that argument it is useful

to present further more complete and very recent oxidation data as a function of the Si substrate orientation(12).

The oxidation data of Massoud et al(19-21) has recently been extended down to 600°C(12) where the intrinsic stresses are larger(22-26) and now includes the (311) and (511) orientations as well as the (111), (110), and (100) major Si orientations. The crossover in the thickness time plots between the (110) and (111) orientations has been observed for all oxidation temperatures between 1100°C and 750°C inclusive. For lower oxidation temperatures, the films were not grown thick enough to exhibit a crossover in the thickness time plots, but a crossover in the oxidation rates (the slope of the thickness-time plots) was observed. The (311) and (511) orientations were originally added to the study because they were thought to have a higher areal density of Si atoms, if one assumes that the planes are flat. However, this assumption was found to be erroneous(27). The (311) and (511) are both vicinal planes of the (100) and (111) planes. This is shown in two dimensions to simplify the situation with the aid of Figure 4 in which the angle for the (311) and (511) planes are made using combinations of the (100) terraces and (111) risers. Using the appropriate ratios of (100) and (111) planes the actual areal densities of Si atoms on the various surfaces are calculated(12,28) and shown in Table 3. The oxidation data at 700°C and 1000°C are shown in Figure 5. A crossover in only the oxidation rate is obtained for the lower temperature, since the data have not been carried out to

sufficient SiO_2 thicknesses to observe the crossover on the thickness-time plot. For the 1000°C data the crossover is noticed on the plot. For the three major orientations the crossover has been reported(19-22) and is shown in Figure 6 for an 800°C oxidation. In the pre crossover regime the rate order is:

$$\text{Rate}(110) > \text{Rate}(111) > \text{Rate}(311) > \text{Rate}(511) > \text{Rate}(100)$$

This order parallels the order for the number of Si atoms as given in Table 3, but agreement is not quantitative. Table 4 shows a comparison for the 700°C and 1000°C data and while agreement is better at the higher temperatures quantitative agreement with N_s is lacking. At the present time a proven model that both explains the crossover and is quantitative is not available. However, a proposal will be offered which appears consistent with the available data and the steady state ideas presented above.

For an explanation of the crossover, we return to a steady state diagram shown in Figure 7 which is similar to Figure 2 with the addition of some new flux lines. On the right of the diagram the two different lines represent different interfacial fluxes due to the different N_s , for the (110) and (111) Si surfaces. From equation (2), $k[\text{Si}]$ is different according to the N_s . On the left is an additional flux line representing the effect of increased compressive stress for all the orientations except the (111) which shows the smallest stress. A compressive film stress

decreases D for the film, thereby decreasing the F intercept and the slope. The effect is a decrease in the observed flux, i.e. the oxidation rate, as indicated on the figure by a flux line intersection at a lower F for the (110) plane relative to the (111) Si surface. The stress effect on the oxidation rate increases as the film grows, because the resultant force increases with film thickness. Since the effect of stress on the oxidation flux or D is not yet quantitative, we only obtain the direction for the change. Thus the reduced stress on the (111) or the increased stress on the other orientations causes a corresponding increase in D for the (111) or decrease for the other orientations. This stress change causes a change in the steady state position and hence the observed oxidation rate crossover.

In summary then the steady state analysis can yield a reasonable if not yet quantitative idea of the various oxidation parameters.

Photonic Effects

A number of recent studies have pointed out that both thermal and photonic effects are at play when oxidation is performed in the presence of high intensity light(29-34). There exists evidence that photon energies greater than 3 eV yield large oxidation rate enhancements(30,34). From the energy band picture for the Si-SiO₂ interface, as seen in Figure 8, about 3 eV is the energy distance from the Si conduction band to the SiO₂

conduction band. Further oxidation rate enhancements were observed for photon energies greater than 5 eV which corresponds to the dissociation energy for the O_2 molecule. It thus appears that electron excitation plays a significant role in the oxidation of Si, in addition to the chemical effects of [O] and [Si] in the traditional oxidation model.

Silicide Oxidation Studies

The role of electrons on the Si surface is further substantiated from recent studies of the oxidation behavior of a variety of metal silicides. Firstly, new oxidation data are presented. A variety of metal silicides were cleaned(35) and oxidized so as to produce only SiO_2 and preserve the silicide. This can be accomplished in the appropriate temperature regime (about 800°C) and most importantly with the silicides deposited upon a Si substrate which insures a supply of Si for the oxidation reaction, such that the silicide can be preserved. Thus there is a net flux of Si from the substrate to the silicide- SiO_2 interface and a net flux of metal towards the Si. The actual flux may be more complicated and found to be different for different silicides(36-39). The results of dry O_2 oxidations at 800°C are shown in Figure 9(40). Three bands of oxidation behavior are characteristic: the fastest oxidizing silicides are the transition metal silicides; the intermediate oxidizing silicides are the refractory silicides; the slowest are the semiconducting silicides which display oxidation rates not much different from

Si itself. It was also found that the free carrier concentrations and the optical absorption index, κ , which is related to the free carrier concentration, all display the same order as the oxidation rate. In addition is a report(41) that Si surfaces that have a comparatively large density of electron states near the Fermi level oxidize comparatively rapidly. These experiments were done under UHV conditions using disordered (high density of states) and ordered (low density of electron states) noble metal sub-monolayers on single crystal Si substrates. Taken together these experimental findings point to a profound oxidation rate enhancement effect due to the high electron densities. This is in further corroboration to the photonic results above.

A Thermionic Emission Model For Si Oxidation

Referring back to Figure 8, and now considering the importance of electron availability, a straightforward dependence of the availability of electrons, as the electron flux, $F_{e,}$, on the oxidation rate can be tested(42) using the thermionic emission relationship, viz. the Richardson-Dushman equation:

$$F_{e,} = AT^2 \exp(-\chi_0/kT) \quad (8)$$

where A is the Richardson constant, T is absolute temperature, χ_0 is the barrier height which, as typically applied to metals, extends from the Fermi level of the metal to vacuum. For the present case of electron emission from Si to SiO_2 , we consider

the highest levels in Si that have sufficient electrons to supply the oxidation reaction. Calculations have shown that there are more than sufficient O_2 molecules on the SiO_2 side of the interface as a result of a fast diffusive flux, and more than sufficient electrons available on the Si side(42). Thus the rate limiting step is assumed to be emission of electrons over the barrier, step 2 below, and the entire oxidation reaction is envisioned as follows:

1. e^- (C.B. of Si) \rightarrow e^- (Si surface)
2. e^- (Si surface) \rightarrow e^- (free in SiO_2)
3. e^- (in SiO_2) + O_2 (from diffusion) \rightarrow O_2^-
4. $O_2^- \rightarrow O + O^-$
5. Si^+ (Si surface) + $O + O^- \rightarrow SiO_2$

Steps 1, 3-5 are relatively fast with respect to step 2. Step 1 represents the flux of electrons to the Si surface. Step 3 represents the thermodynamically favored process of electron attachment to O_2 (43). This step destabilizes O_2 and leads to decomposition to a neutral and charged O species(43). Then step 5 considers the rapid reaction of the atomic and charged species. Notice that Si is represented as Si^+ , since electrons were lost from the surface.

One way to test the rate limitation of Step 2 is to equate the thermionic emission electron flux, F_e , with the observed oxidation flux, $F(\text{exp})$, as an SiO_2 flux, and then calculate the

value of χ_0 necessary for the equivalency, and compare this with the energy band diagram and known values for the various barriers. Table 5 reports these χ_0 values obtained from oxidation data at various temperatures and for the Si (110) and (100) orientations. These orientations represent the fastest and slowest oxidizing surfaces in the initial regime. Also while the initial oxidation rates were emphasized, since thermionic emission is expected to control the very initial rate, larger thicknesses were included to show trends. It is seen that within a few tenths of an eV the value of 3 eV is obtained for χ_0 which corresponds to the barrier between the Si conduction band and SiO_2 , thus confirming the models consistency. It is easily verified that the Si conduction band contains sufficient electrons to supply the oxidation reaction at any temperatures above 100°C . At room temperature it is universally observed that a thin native oxide film forms on freshly etched or cleaved Si surface with a thickness that may range from 5 to 20 Å. Thermionic electrons do not seem available for this process. However, when the $\sim 10^{15}$ cm^{-2} surface electron states on the Si surface are considered, an explanation emerges. If each of these states can contribute a trapped electron to oxidation, as the state is removed via oxidation, then this number of electrons would explain the formation of about 10 Å SiO_2 , considering one electron per SiO_2 molecule as per the reaction scheme above via electron attachment to O_2 . This mechanism would cease once the states are destroyed, as is observed for the formation of the

native oxide. Then the thermionic supply function is invoked to continue the oxidation at higher temperatures. After the initial regime the reaction mechanism may be controlled by other processes which would shift the steady state point as discussed above. A thickness dependent thermionic emission does not seem plausible.

Summary and Conclusions

Several new ideas and experimental results were discussed pertaining to Si oxidation, especially in the initial oxidation regime. Many of these ideas have only recently or not yet appeared in the literature.

One recent study clearly linked the Si oxidation rate to the areal density of Si atoms on the Si surface, N_s . This dependence existed to surprisingly large oxide thicknesses of several thousands of Å. Using recent intrinsic SiO₂ stress measurements, the oxidation rate crossover phenomena between the (110) and (111) orientations was explained. This was understood using pictorial representations of the essential fluxes for the oxidation process, and the steady state solution for the fluxes in a series process. New results for the oxidation of metal silicides to produce SiO₂ films along with recently reported photonic effects on Si oxidation have pointed to the importance of electron supply to the Si oxidation mechanism. A simple analysis of the initial oxidation rates in terms of a thermionic

emission model yielded correct values for the Si-SiO₂ barrier.

Quantitative aspects of several of the presented ideas are still lacking and require more research. The area of potential electronic implications of these new studies has not been addressed in the paper, but such relationships likely exist. For example, the origin of interface fixed charge may be explained by the emission of electrons into SiO₂ during oxidation. Continuing research at our laboratory focuses on quantification of the results and the experimental verification of possible relationships between materials parameters and electronics properties of the Si-SiO₂ interface.

Acknowledgements

The authors are deeply indebted to R.D. Frampton, F.M. d'Heurle, E. Kobeda, and E.A. Lewis for access to their recent data and for helpful discussions. This research was sponsored in part by the Office of Naval Research, ONR.

References

1. U.R. Evans, "The Corrosion and Oxidation of Metals," Edward Arnold Ltd., London (1960).
2. W.A. Pliskin, IBM J. Res. Dev., 10, (1966) 198.
3. B.E. Deal and A.S. Grove, J. Appl. Phys., 36, (1965), 3770.
4. A.G. Revez, K.H. Zaininger, R.J. Evans, J. Electrochem. Soc., 113, (1966), 706.
5. E. Rosencher, A. Straboni, S. Rigo and G. Amsel, Appl. Phys. Lett., 34, (1979), 254.
6. S. Rigo, F. Rochet, B. Agius and A. Straboni, J. Electrochem. Soc., 129, (1982) 867.
7. R. Pfeffer and M. Ohring, J. Appl. Phys., 52, (1981) 777.
8. E.A. Irene, J. Electrochem. Soc., 121, (1974) 1613.
9. E.A. Irene and R. Ghez, J. Electrochem. Soc., 124, (1977) 1757.
10. R.J. Zeto, C.G. Thornton, E. Hryckovian and C.D. Bosco, J. Electrochem. Soc., 122, (1975) 1410.
11. L.N. Lie, R.R. Razouk and B.E. Deal, J. Electrochem. Soc. 129, (1982) 2828.
12. E.A. Lewis and E.A. Irene, J. Electrochem. Soc., in press 1987.
13. E.A. Irene, Phil. Mag.B., 55, (1987) 131.
14. F.J. Norton, Nature, 191, (1961) 701.
15. W.A. Tiller, J. Electrochem. Soc., 127, (1980) 625.
16. J.R. Ligenza, J. Phys. Chem., 65, (1961) 2011.
17. S.I. Raider and L.E. Forget, J. Electrochem. Soc., 127, (1980) 1783.
18. E.A. Irene, J. Electrochem. Soc., 121, (1974) 1613.
19. H.Z. Massoud, J. Plummer and E.A. Irene, J. Electrochem. Soc., 132, (1985) 1745.
20. H.Z. Massoud, J.D. Plummer and E.A. Irene, 132, (1985) 2686.
21. H.Z. Mazzoud, J.D. Plummer and E.A. Irene, 132, (1985) 2693.

22. E.A. Irene, H.Z. Mazzoud and E. Tierney, J. Electrochem. Soc. 133, (1986) 1253.
23. E. Kobeda and E.A. Irene, J. Vac. Sci. Technol. B, 4, (1986) 720.
24. E. Kobeda and E.A. Irene, J. Vac. Sci. Technol. B, 5, (1987) 15.
25. E.P. EerNisse, Appl. Phys. Lett., 30, (1977) 290; 35, (1979) 8.
26. E.A. Irene, E. Tierney and J. Angillelo, J. Electrochem. Soc. 129, (1982) 2594.
27. K. Ueda and M. Inoue, Surf. Sci., 161, (1985) L578.
28. E.A. Lewis, K. Kobeda and E.A. Irene, "Proceedings of Fifth International Symposium on Silicon Materials Science and Processing," Ed. H.R. Huff, Boston, Mass., May 1986.
29. S.A. Schafer and S.A. Lyon, J. Vac. Sci. Technol., 19, (1981) 494.
30. S.A. Schafer and S.A. Lyon, J. Vac. Sci. Technol., 21, (1982) 422.
31. Ian W. Boyd, Appl. Phys. Lett., 42, (1983) 728.
32. Ian W. Boyd, "Surface Studies with Lasers," Eds. F.R. Aussenberg, A. Leitner and M.E. Lippitech, Springer-Verlag (1983) p. 193.
33. E.M. Young and W.A. Tiller, Appl. Phys. Lett., 42, (1983) 63.
34. E.M. Young and W.A. Tiller, Appl. Phys. Lett., 50, (1987) 80.
35. R.D. Frampton, E.A. Irene, J. Appl. Phys. 59, (1986) 978.
36. F.M. d'Heurle, A. Cros, R.D. Frampton and E.A. Irene, Phil. Mag. B, 55, (1987) 291.
37. F.M. d'Heurle, in "Solid State Devices 1985," ed. P. Balk and O.G. Folberth, Elsevier, Amsterdam, (1986) p. 213.
38. H. Jiang, C.S. Peterason and M.A. Nicolet, Thin Solid Films, 140, (1986) 115.
39. S.P. Murarka, "Silicides for VLSI Applications," Academic Press, New York (1983).
40. R.D. Frampton, E.A. Irene and F.M. d'Heurle, J. Appl. Phys.,

submitted for publication 1987.

41. A. Cros, J. de. Phys, 44, (1983) 707.

42. E.A. Irene and E.A. Lewis, Appl. Phys. Lett., submitted for publication 1987.

43. L.M. Chanin, A.V. Phelps and M.A. Biondi, Phys. Rev., 128, (1962) 219.

44. V.G. Levich, "Physicochemical Hydrodynamics", Prentice Hall Inc., Englewood Cliffs, New Jersey., 1962 p72-78.

List of Figures

- Figure 1. The essential rate processes for Si oxidation: F_1 is the flux of oxidant; and F_2 the reaction between Si and oxidant.
- Figure 2. A flux diagram showing the variation of F_1 and F_2 with C_0 , the concentration of oxidant at the Si-SiO₂ interface.
- Figure 3. Intrinsic SiO₂ film stress as a function of oxidation temperature and Si substrate orientation (ref. 24, with permission of the Am. Vac. Soc.).
- Figure 4. A two dimensional view of (311) plane relative to (100) and (111) displaying the stepped nature of the (311) surface.
- Figure 5. Oxidation data for five Si orientations at a) 700°C and b) 1000°C (ref. 12 with permission of the Electrochem. Soc.).
- Figure 6. Oxidation data at 800°C for three major orientations, ((110) triangles, (111) squares, (100) circles) a) a close up of the initial data prior to crossover and b) after the crossover (ref. 22 with permission of Electrochem. Soc.).
- Figure 7. Flux versus C_0 for the (110) and (111) Si orientations, F_2 's, and for two different D values, F_1 's.
- Figure 8. Energy band diagram for Si-SiO₂ interface showing the barrier of about 3.15eV from the bottom of the Si conduction band.
- Figure 9. Oxidation data for a variety of metal silicides (ref. 40).

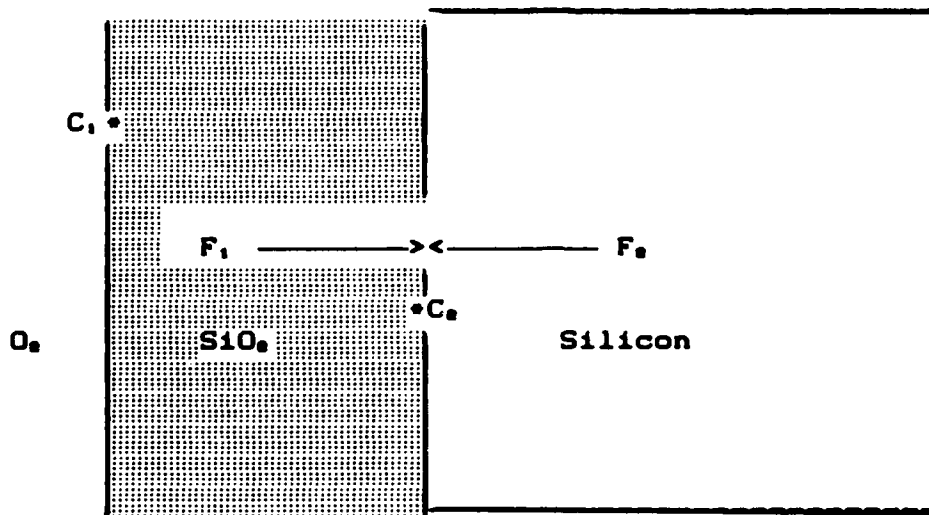
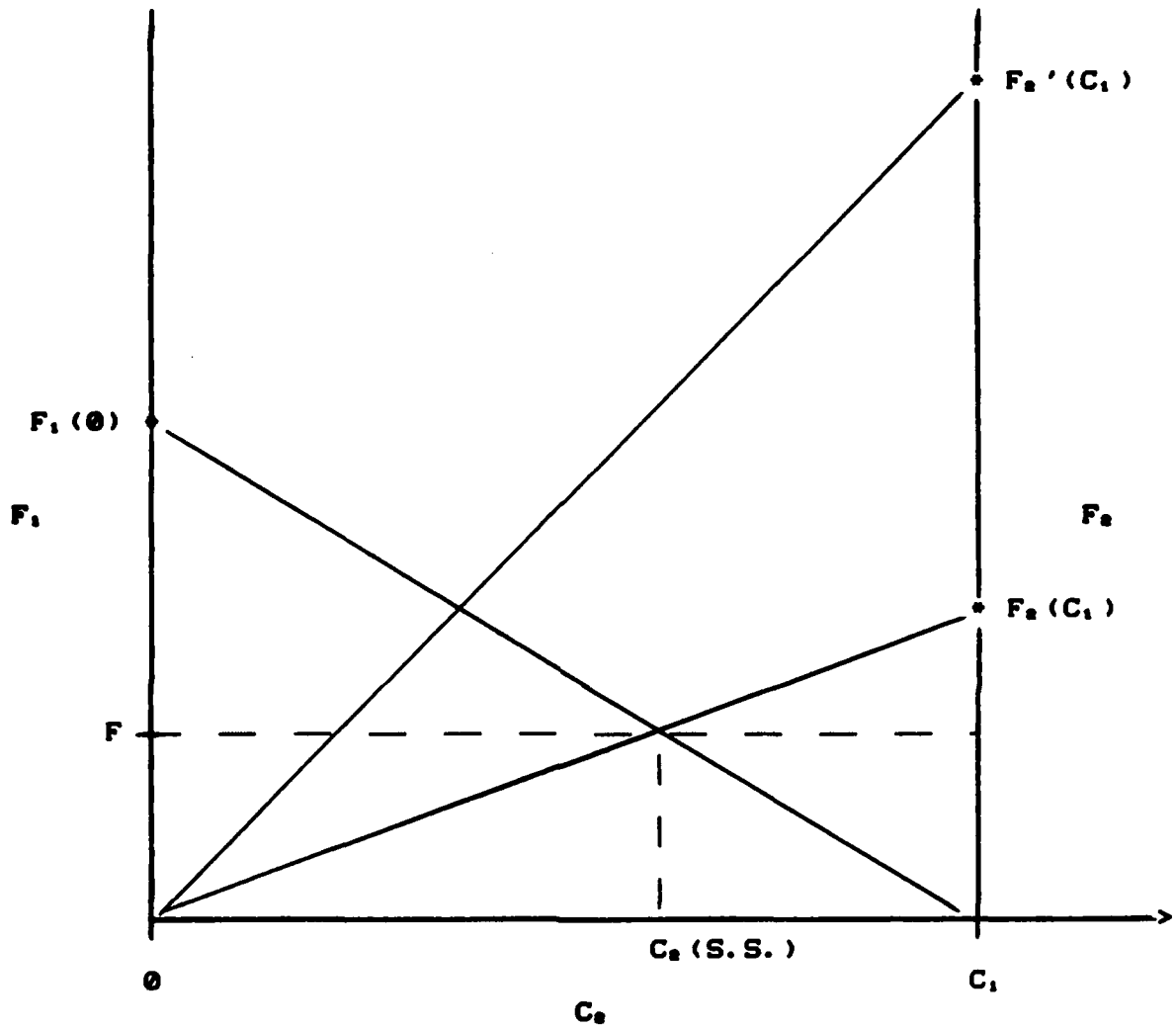


Fig 1 Irene

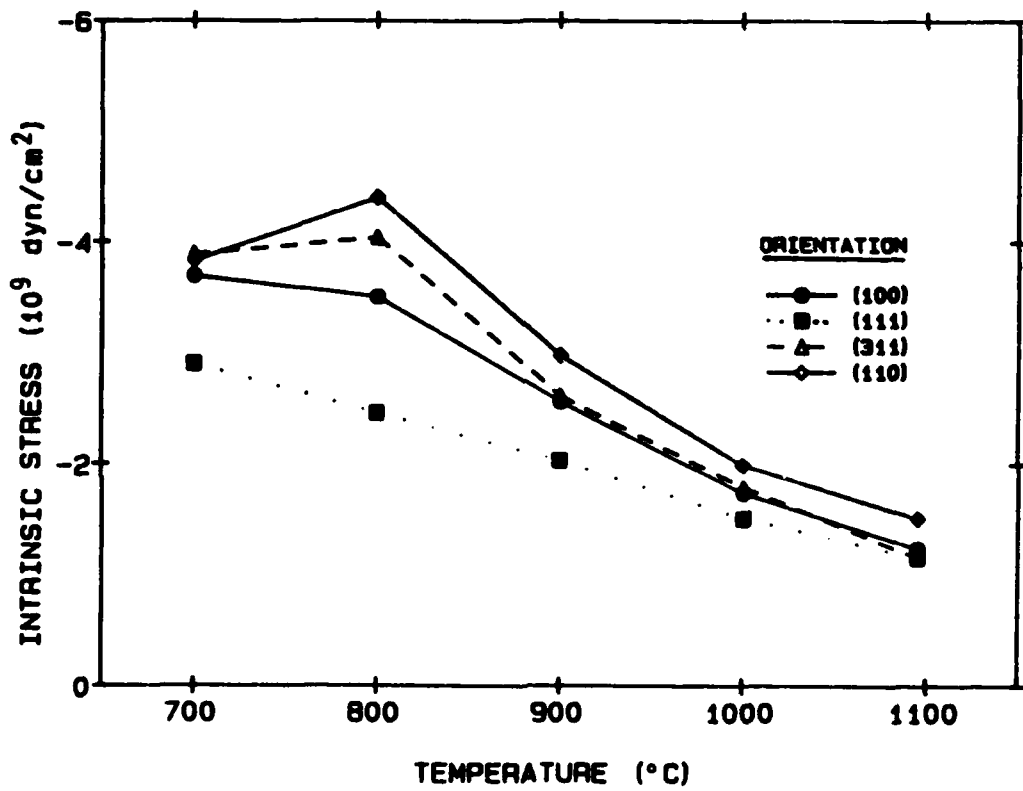


$$F_1 = D(C_1 - C_2)/L$$

$$F_2 = k[S_1][O_2] = kN_{O_2}C_2$$

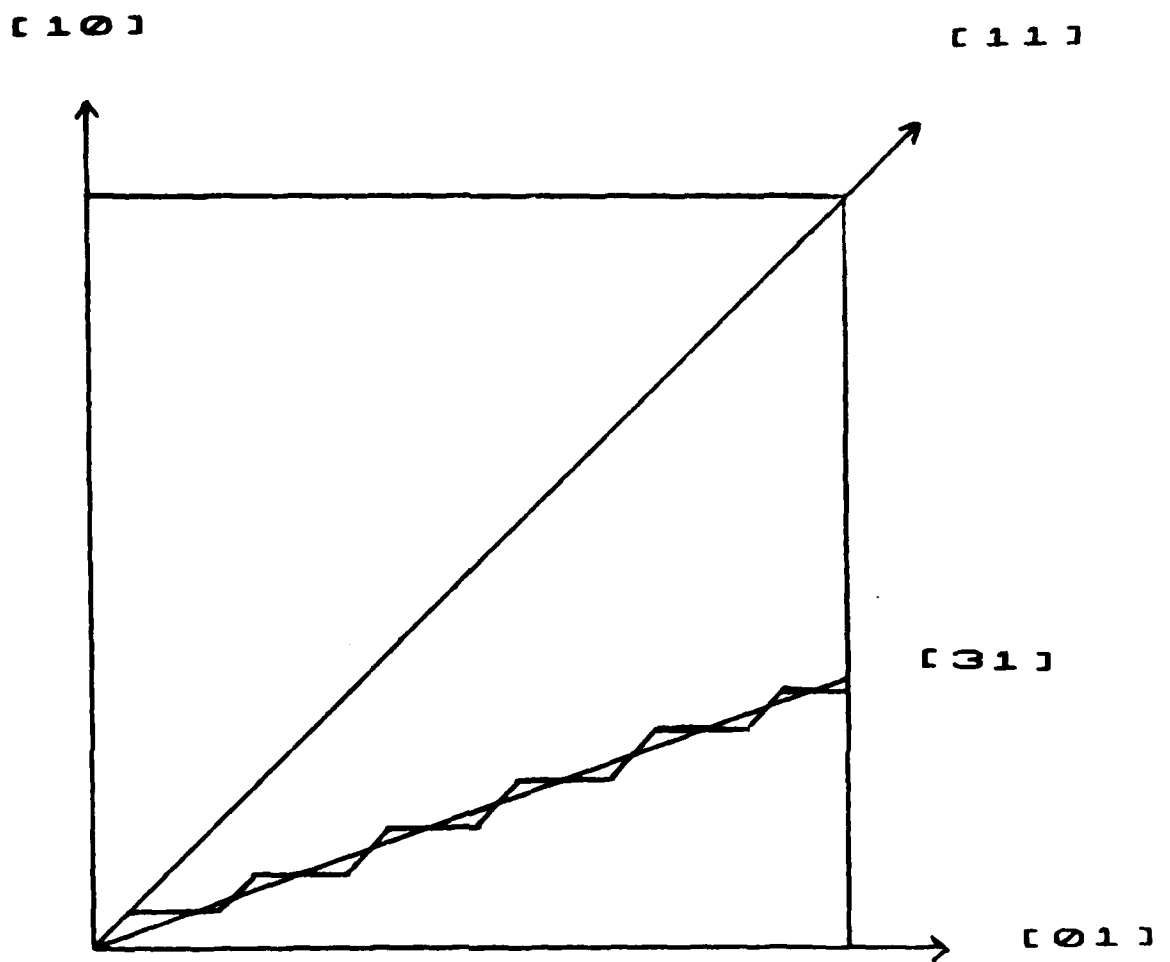
$$F = F_1 = F_2$$

Irene Fig 2.



Irene Fig 3.

(31) As Vicinal Plane



- (11) Risers**
- (10) Terraces**

Fig 4 Irene

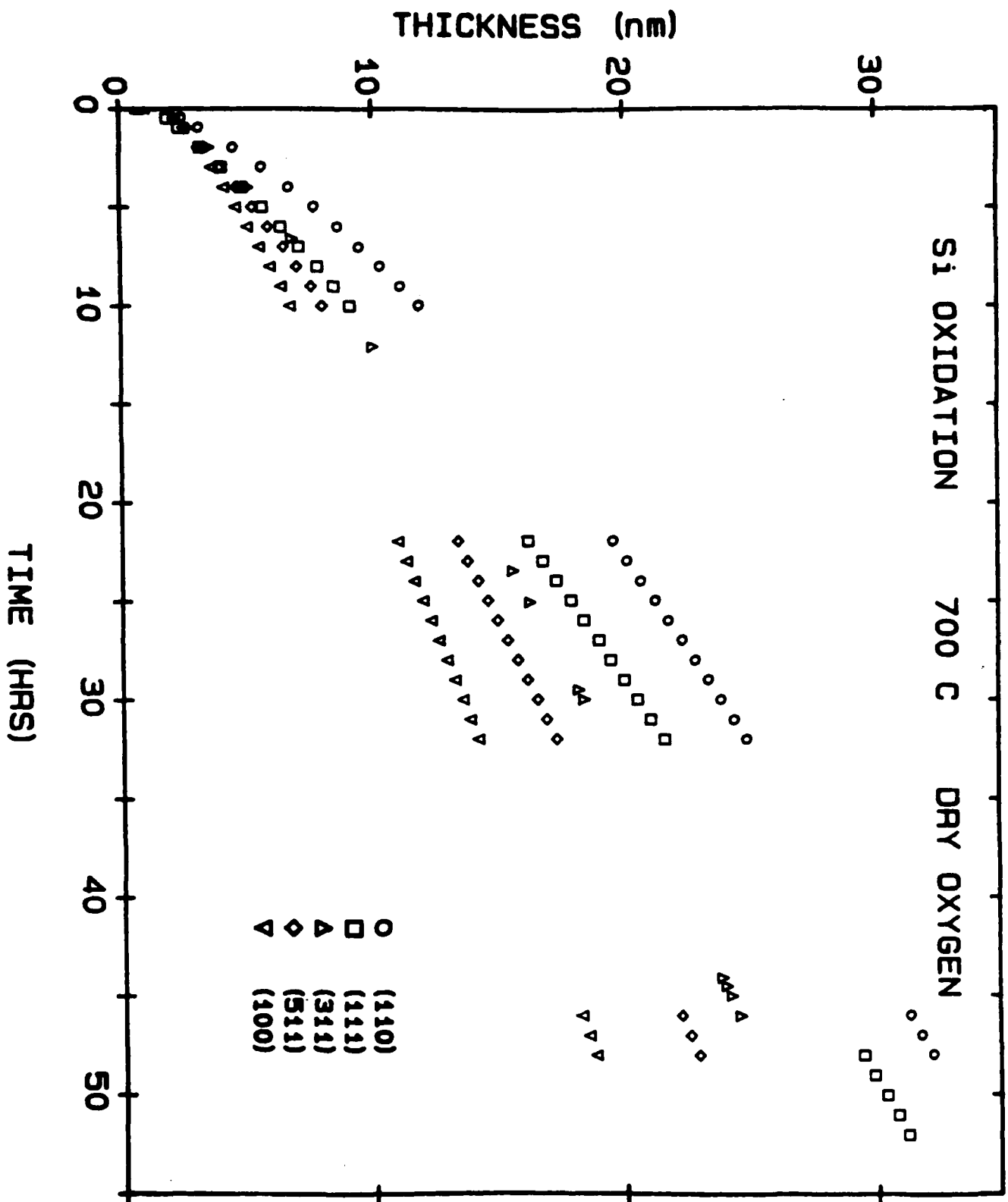
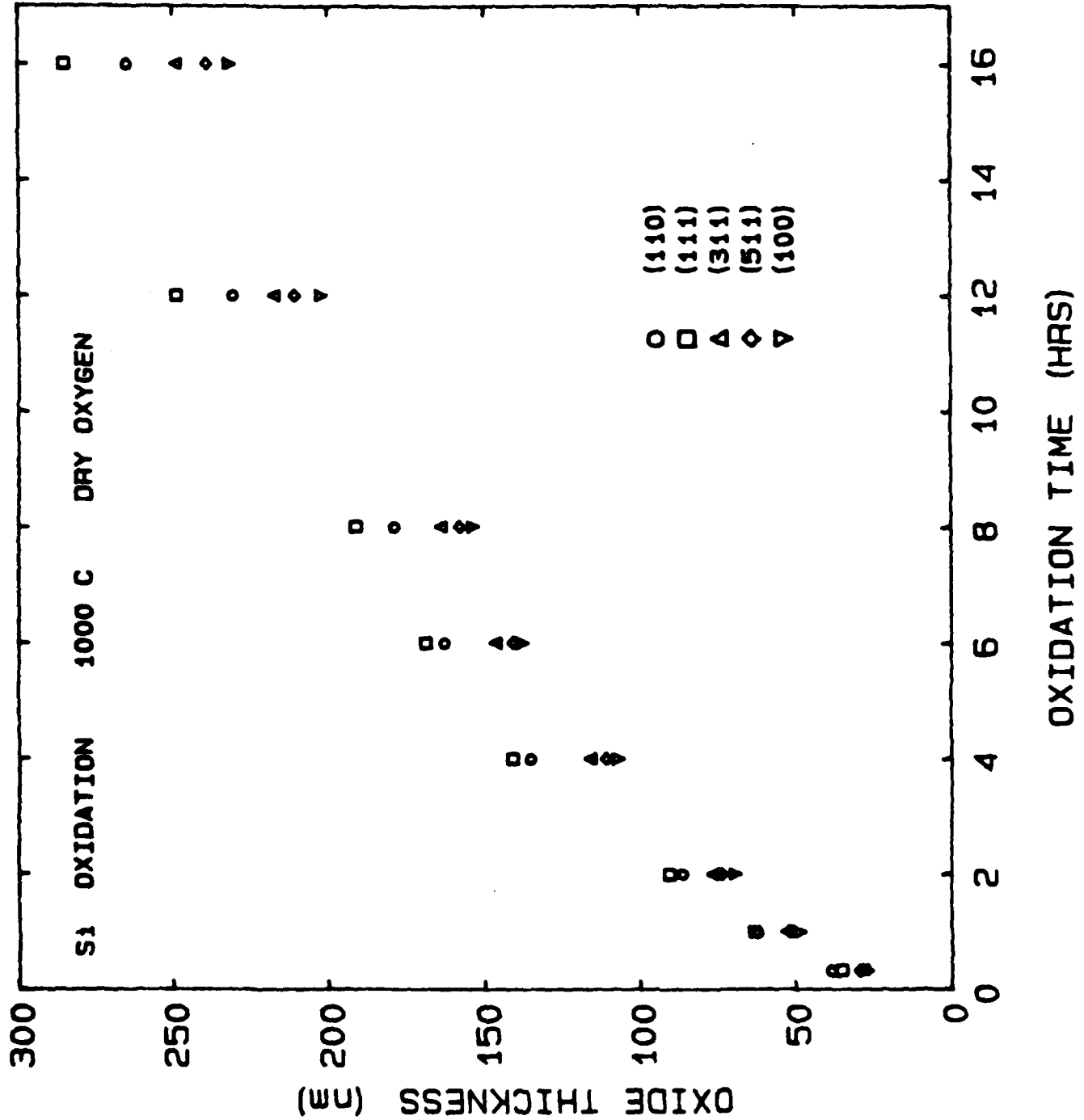


Fig 5a Irene

Fig 5 6
Irene



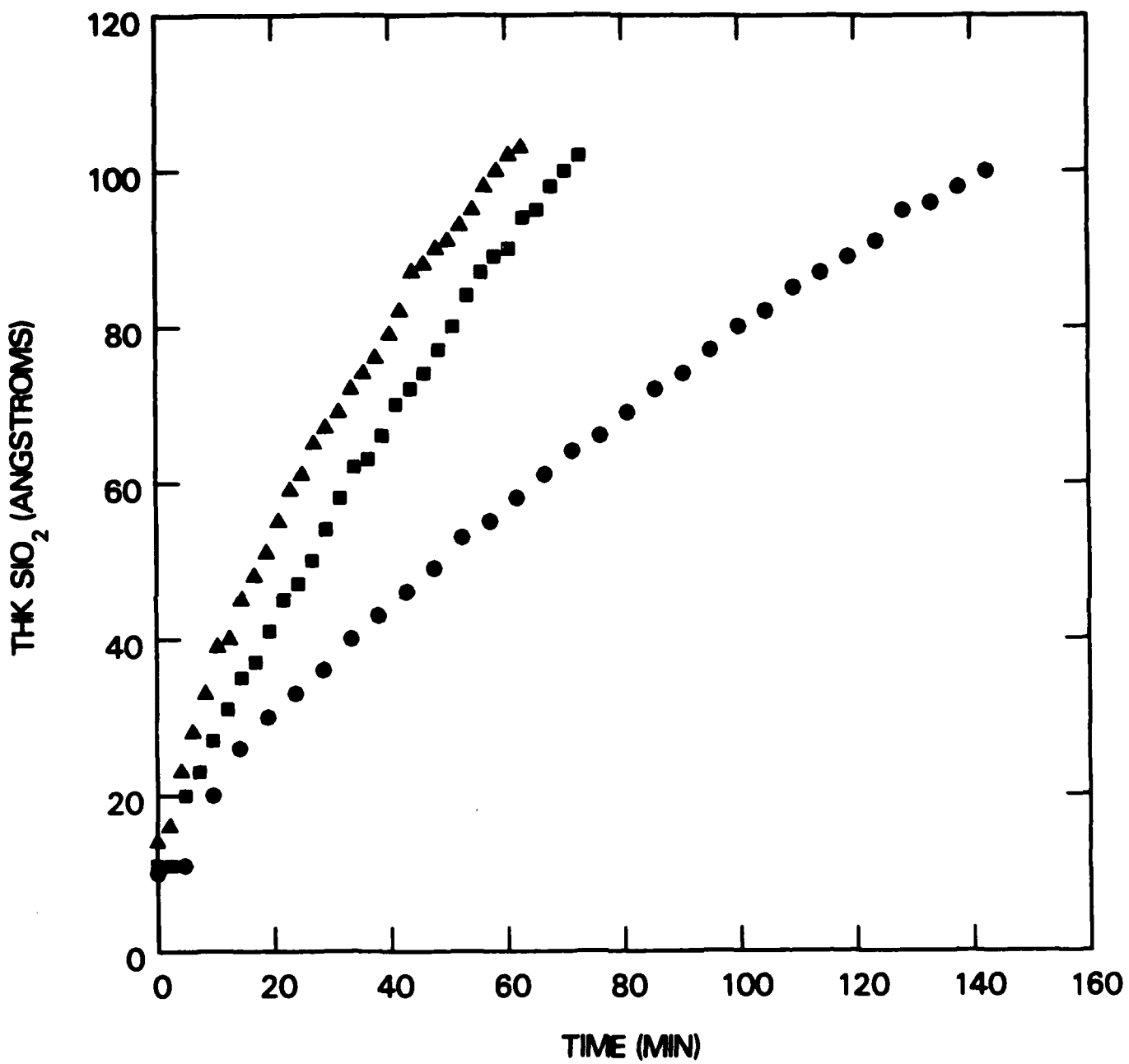


Fig 6a Irene

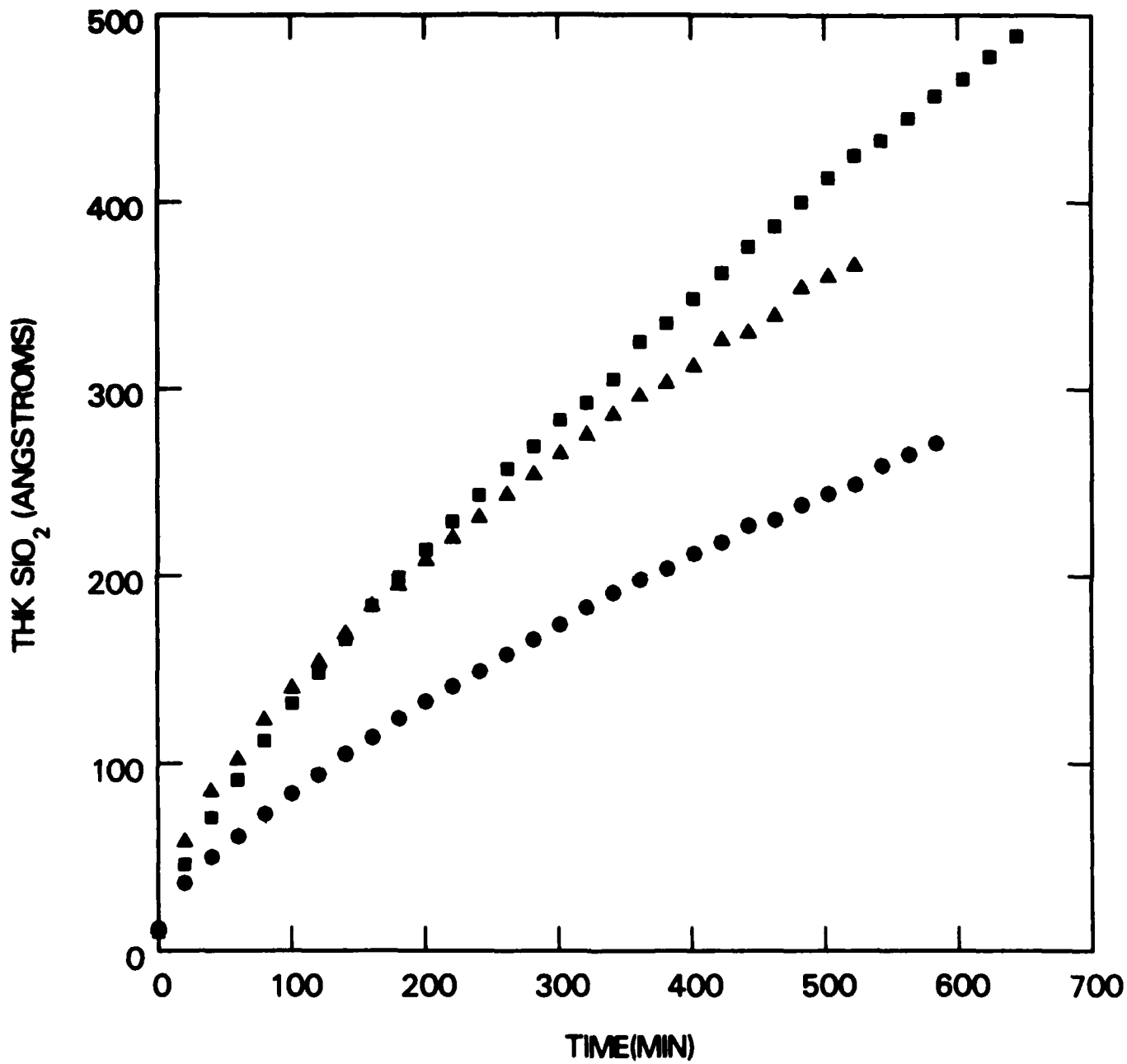
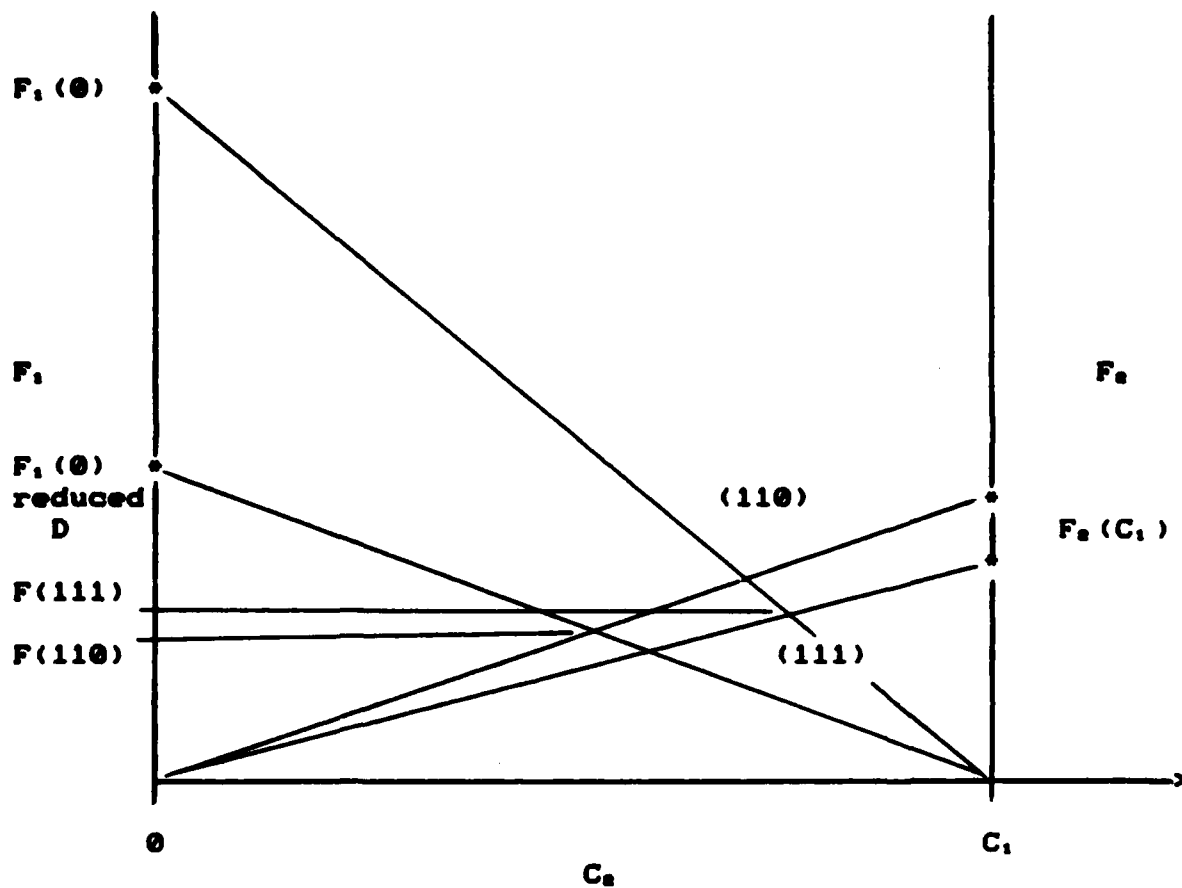


Fig 6 b Irene



F_2 for the (110) and (111) orientations
 $F_2(110) > F_2(111)$

F_1 reduced by Stress on (110)

Crossover:
 $F(111) > F(110)$

Fig 7 Irene

Vacuum Level

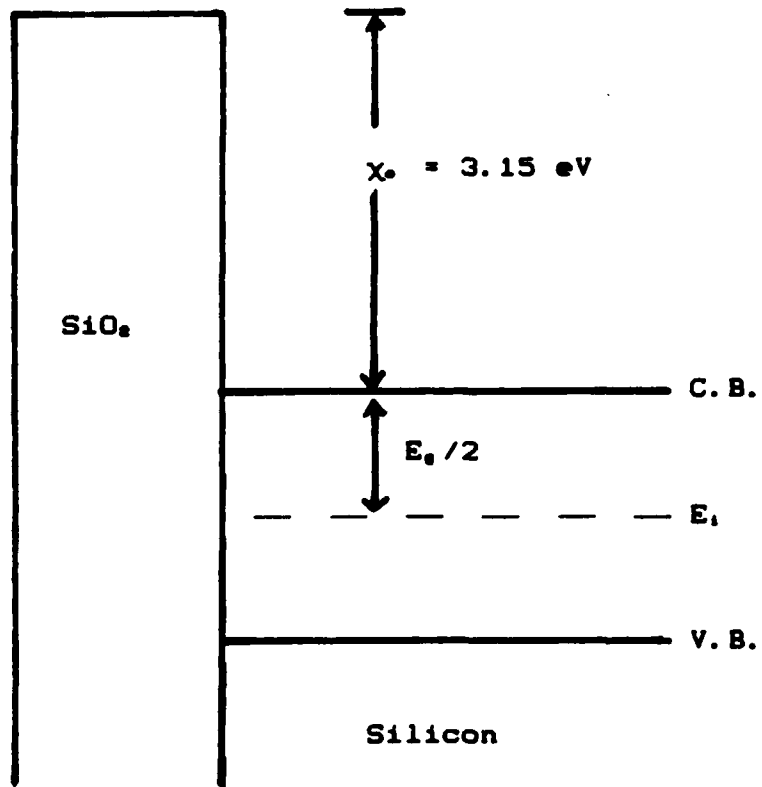


Figure 8 Irene

Fig. 9. Irene

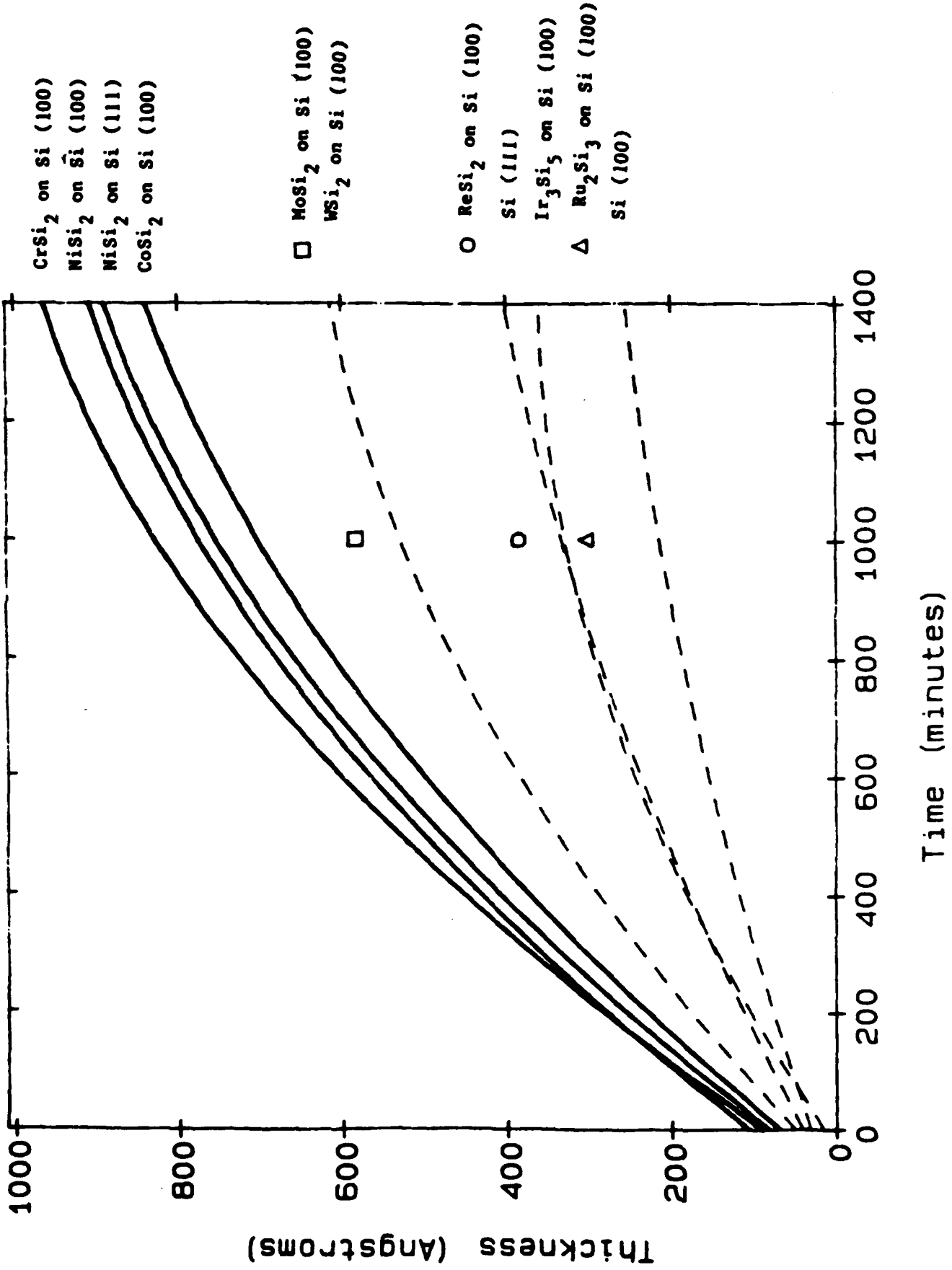


Figure 6. Ex situ Oxidation Results at 750°C

END

7-87

DITIC